Mutation Research - Genetic Toxicology and Environmental Mutagenesis xxx (xxxx) 503446

Contents lists available at ScienceDirect

Mutation Research - Genetic Toxicology and Environmental Mutagenesis

journal homepage: www.elsevier.com/locate/gentox

A comparative study of persistent DNA oxidation and chromosomal instability induced *in vitro* by oxidizers and reference airborne particles

Xin Cao [a, b], Sara Padoan [a, c], Stephanie Binder [a, b], Stefanie Bauer [a], Jürgen Orasche [a], Corina-Marcela Rus [b, d], Ajit Mudan [c], Anja Huber [a], Evelyn Kuhn [a], Sebastian Oeder [a], Jutta Lintelmann [e], Thomas Adam [a, c], Sebastiano Di Bucchianico [a, *], Ralf Zimmermann [a, b]

[a] Joint Mass Spectrometry Center, Comprehensive Molecular Analytics, Helmholtz Zentrum München, Neuherberg, Germany
[b] Joint Mass Spectrometry Center at Analytical Chemistry, Institute of Chemistry, University of Rostock, Rostock, Germany
[c] Institute of Chemistry and Environmental Engineering, University of the Bundeswehr Munich, Neubiberg, Germany
[d] Centogene GmbH, Rostock, Germany
[e] Research Unit of Molecular Endocrinology and Metabolism, Helmholtz Zentrum München, Neuherberg, Germany

ARTICLE INFO

Keywords:
Oxidative DNA damage
Genotoxicity
Micronuclei
Reference particulate matter
Oxidizing agents

ABSTRACT

Adverse health effects driven by airborne particulate matter (PM) are mainly associated with reactive oxygen species formation, pro-inflammatory effects, and genome instability. Therefore, a better understanding of the underlying mechanisms is needed to evaluate health risks caused by exposure to PM. The aim of this study was to compare the genotoxic effects of two oxidizing agents (menadione and 3-chloro-1,2-propanediol) with three different reference PM (fine dust ERM-CZ100, urban dust SRM1649, and diesel PM SRM2975) on monocytic THP-1 and alveolar epithelial A549 cells. We assessed DNA oxidation by measuring the oxidized derivative 8-hydroxy-2'-deoxyguanosine (8-OHdG) following short and long exposure times to evaluate the persistency of oxidative DNA damage. Cytokinesis-block micronucleus cytome assay was performed to assess chromosomal instability, cytostasis, and cytotoxicity. Particles were characterized by inductively coupled plasma mass spectrometry in terms of selected elemental content, the release of ions in cell medium and the cellular uptake of metals. PM deposition and cellular dose were investigated by a spectrophotometric method on adherent A549 cells. The level of lipid peroxidation was evaluated via malondialdehyde concentration measurement. Despite differences in the tested concentrations, deposition efficiency, and lipid peroxidation levels, all reference PM samples caused oxidative DNA damage to a similar extent as the two oxidizers in terms of magnitude but with different oxidative DNA damage persistence. Diesel SRM2975 were more effective in inducing chromosomal instability with respect to fine and urban dust highlighting the role of polycyclic aromatic hydrocarbons derivatives on chromosomal instability. The persistence of 8-OHdG lesions strongly correlated with different types of chromosomal damage and revealed distinguishing sensitivity of cell types as well as specific features of particles versus oxidizing agent effects. In conclusion, this study revealed that an interplay between DNA oxidation persistence and chromosomal damage is driving particulate matter-induced genome instability.

Abbreviations: PM, particulate matter; CZ100, fine dust ERM-CZ100; UD 1649, urban dust SRM1649; diesel PM2975, diesel PM SRM2975; 3-MCPD, 3-chloro-12-propanediol; 8-OHdG, 8-hydroxy-2'-deoxyguanosine; PAHs, polycyclic aromatic hydrocarbons; MAPK, mitogen-activated protein kinase; MDA, malondialdehyde; NF-κB, nuclear factor κB; AP-1, activator protein 1; MN, micronuclei; NPB, nucleoplasmic bridge; NBUD, nuclear bud; ROS, reactive oxygen species; EMS, ethyl methanesulfonate; FBS, fetal bovine serum; PBS, phosphate buffered saline; DMSO, dimethyl sulfoxide; dG, 2'-deoxyguanosine; TE buffer, tris-EDTA buffer; SPE, solid phase extraction; LC-MS/MS, liquid chromatography tandem mass spectrometry; MRM, multiple reaction monitoring; LC-UV, liquid chromatography ultraviolet detection; CBMN Cyt assay, cytokinesis-block micronucleus cytome assay; SEM, standard error of mean; CBPI, cytokinesis-block proliferation index; MI, mitotic index; mono, mononucleated cells; BN, binucleated cells; CYP1A1, cytochrome P450 family 1 subfamily A polypeptide 1

* Corresponding author.
E-mail address: dibucchianico@helmholtz-muenchen.de (S. Di Bucchianico).

https://doi.org/10.1016/j.mrgentox.2022.503446
Received 20 September 2021; Received in revised form 29 November 2021; Accepted 10 January 2022
1383-5718/

1. Introduction

A number of studies have linked airborne particulate matter (PM) exposure with a wide range of human diseases including cardiopulmonary failure, type II diabetes mellitus, neurological disorders and cancer [1,2,3]. PM-induced adverse effects involve oxidative stress and inflammation, which in turn may lead to different genetic alterations [4]. DNA damage and repair play a pivotal role in the pathogenesis of asthma and the telomeric erosion caused by oxidative stress was proven as a mechanism underlying PM related cardiovascular disease [5,6]. Particularly in susceptible populations, PM is an important environmental factor that exacerbates inflammatory processes by cellular responses to PM-induced oxidative stress [7]. It is widely recognized that the adverse health effects of PM exposure are mediated by oxidative stress and the induction of inflammation is mediated by signaling pathways (e.g. MAPK) and transcription factors (e.g. NF-κB, AP-1) [8]. Airborne PM contains a complex mixture of toxic compounds – including polycyclic aromatic hydrocarbons (PAHs), their derivatives such as nitrated PAHs (nitro-PAHs) and transition metals – and it is composed of different size fractions that may induce diverse toxic mechanisms of action and effects. While the PAHs compounds in PM can form stable bulky DNA adducts, which inhibit DNA replication and transcription, metals primarily act as oxidizing agents inducing 8-hydroxy-2'-deoxyguanosine (8-OHdG) formation as well as DNA single and double strand breaks [9,10,11].

Chromatin is a dynamic entity that responds to environmental cues in terms of structure and function and its organization may be disrupted inter alia by, for example, the formation of DNA strand breaks. Failure of subsequent repairing processes and cell cycle checkpoints may lead to mutations and chromosomal rearrangements that result in phenotypic changes or ultimately result in cell death [12,13]. In particular, DNA double strand breaks are considered as a critical primary lesion for the formation of chromosomal aberrations [14]. In this context, the present study aimed at investigating the correlation between PM-induced persistent oxidative DNA damage, evaluated via measurements of 8-OHdG formation, and chromosomal instability as determined in terms of micronuclei (MN), nucleoplasmic bridges (NPB), and nuclear buds (NBUD) induction as well as mitotic dysfunction and cell death. Oxidative stress, considered as the underlying mechanism of PM-induced genotoxicity, was detected by measuring one of the end product of lipid peroxidation, malondialdehyde (MDA). This study also focused on the role of bioavailable metals in PM induced toxic effects versus the total PM metal content. For this scope, nine elements, namely vanadium, chromium, manganese, iron, nickel, copper, zinc, arsenic, cadmium, and lead were determined by inductively coupled plasma mass spectrometry (ICP-MS) in PM samples. Additionally, relative levels of those metals were determined intra- and extracellularly following cell exposures to reference PM.

To address the role of different PAHs and metals in driving persistent oxidative DNA damage and subsequent chromosomal instability on different functional levels, two cell models were used: human monocytes THP-1 and alveolar epithelial A549 cell lines. Monocyte-like THP-1 cells represent an immune-competent cell model to elucidate the influence of immunological mechanisms on particles induced toxicity [15]. The widely used A549 type II pulmonary epithelial cells may give rise to a better understanding of particle-induced mutagenicity/carcinogenicity on lung cells, which is associated with oxidative stress and chromosomal instability. To study the variability of biomarkers for genetic toxicology, which are potentially induced by different ambient PM with diverse chemical identity and similar size distribution, three standard reference materials (SRM) were chosen: i) fine dust ERM-CZ100 (referred to as CZ100 in this paper); ii) urban dust SRM 1649 (UD 1649); iii) diesel PM SRM 2975 (diesel PM). CZ100 consisted of road dust collected in a tunnel in Poland and was released in 2010. It is rich in metals with a similar PAH distribution as UD 1649, an airborne dust from the Washington urban area collected in the late ´70 s. The NIST-certified diesel PM consists of diesel combustion emissions from diesel-powered forklifts and was distributed as diesel reference material since the year 2000. The diesel PM can be characterized as nitro- and alkyl-PAH rich PM mixture. Typically, this diesel PM contains less amount of PAH with five or more condensed aromatic rings (e.g. Benz [a]pyrene). Certified values of certain PAHs and their derivatives are shown in table S1 and the certified elements composition are presented in table S2 of supplementary material.

We compared the effects of the three reference PM with two oxidative and genotoxic substances: menadione and 3-chloro-1,2-propanediol (3-MCPD). Both compounds are known to promote the generation of reactive oxygen species and to induce cellular oxidative stress [16,17]. Possible correlations between the persistence of DNA oxidation and genotoxic endpoints were analyzed by Pearson correlation coefficients.

2. Material and methods

2.1. Materials and reagents

8-OHdG, 2'-deoxyadenosine, 2'-deoxyguanosine monohydrate, thymidine, malondialdehyde tetra butylammonium salt, 2,4-dinitrophenylhydrazine, ammonium acetate, formic acid, 3-chloro-1,2-propanediol, ethyl methanesulfonate, dimethyl sulfoxide, and fine dust ERM-CZ100 were purchased from Sigma (Taufkirchen, Germany). 2'-Deoxycytidine was obtained from Alfa Aesar (Kandel, Germany). Internal standard $^{15}N_5$-8-OHdG and 1,1,3,3-Tetraethoxypropane (1,3-d2) were purchased from Cambridge Isotope Laboratories, Inc. (Massachusetts, USA). Menadione was purchased from AppliChem (Damstadt, Germany). LC-MS grade acetonitrile and methanol were obtained from ChemSolute (Munich, Germany). LC-MS grade water was generated by a Milli-Q Reference System from Merck (Darmstadt, Germany). THP-1 cells were bought from ECACC (No. 88081201). A549 cells were from Leibniz Institute DSMZ (Braunschweig, Germany, ACC 107). LiChrolut® EN 200MG 3 mL cartridges were purchased from Merck (Darmstadt, Germany). Acrodisc® Syringe Filters 13 mm, 0.2 μm GHP were obtained from Waters (New York, USA). Degradase Plus™ were from Zymo Research (Freiburg, Germany). Urban dust SRM1649 and diesel PM SRM2975 were from the National Institute of Standards and Technology (Gaithersburg, USA). N-hexane (GC-grade) was obtained from VWR (Darmstadt, Germany).

2.2. Cell culture, particle exposures, and cell viability

THP-1 and A549 cells were cultured in Roswell Park Memorial Institute medium (supplemented with 10% Fetal Bovine Serum, 2 mM L-glutamine, and 1 % penicillin/streptomycin solution) and incubated at 37 °C, 5% CO_2 in a humidified atmosphere and sub-cultured at 80% confluency. Particulate matter suspension (1 mg/mL) in cell culture medium without FBS were prepared freshly before exposure and dispersed using an ultrasonic bath for 20 min. Menadione and 3-MCPD stock solutions (10 mg/mL) were prepared in DMSO or water, respectively, and diluted in culture medium with FBS before exposure. Concentration-response curves of the tested compounds were made to find the concentration which results in approximately 90% cell viability for subsequent endpoints in order to avoid cytotoxic conditions. THP-1 and A549 cell viability was evaluated using trypan blue dye exclusion after exposure to different concentrations of the test substances for 24 h. Briefly, A549 and THP-1 cells (0.06 and 0.12 million cells/cm^2 in T25 flasks 24 h prior to exposure) were exposed to different concentrations of menadione (0.1-10 μg/mL, 0.2 % DMSO (v/v) final concentration), 3-MCPD (0.1-10 μg/mL), CZ100 (1-1000 μg/mL), UD 1649 (1-1000 μg/mL) and diesel PM (1-100 μg/mL). For the following experiments, 2 μg/mL menadione or 3-MCPD, 200 μg/mL (40 μg/cm^2) of

CZ100 or UD1649, and 40 μg/mL (8 μg/cm^2) of diesel PM were chosen as the concentrations giving rise to approx. 90% cell viability.

2.3. Particle deposition analysis

Particle deposition analysis was performed in adherent A549 cells according to a previous report by Rudd with minor modifications [18]. Briefly, A549 cells (0.06 million cells/cm^2 in T-25 flasks) were seeded 24 h prior the exposure to different PM (200 μg/mL CZ100 or UD 1649 or 40 μg/mL diesel PM) for 48 h in three independent experiments. Cells were washed twice with PBS and collected by centrifugation after trypsinization. The cell pellet was resuspended in 1 mL of 4 N KOH: ethanol (1:1, v/v) by using an ultrasonic bath for 20 min. The suspension was kept in a Thermomixer C (Eppendorf, Germany) at room temperature overnight at 1000 rpm for cell digestion. Afterwards, the suspension was centrifuged at 9390 rcf for 20 min (in 2 mL eppendorf tube). The supernatant was discarded and the pellet was resuspended in 1 mL of water in an ultrasonic bath for 20 min. Finally, the sample absorbance was measured at 748 nm in a Multiskan™ FC Microplate Photometer (Thermo Scientific™, Germany) and the deposited dose was calculated by using standard curves.

2.4. Elemental composition analysis by inductively coupled plasma mass spectrometry (ICP-MS)

Following 48 h exposure to 200 μg/mL of CZ100 or UD 1649, and 40 μg/mL of diesel PM, the cellular uptake of the elements arsenic, cadmium, chromium, vanadium, manganese, copper, nickel, zinc and lead and the release of their respective ions from the particles into cell culture medium was quantified by ICP-MS. At the end of the exposure, cell culture supernatants were collected and A549 and THP-1 cells were harvested and counted. Then, A549 and THP-1 supernatants as well as the collected cells were acidified with a mixture of nitric acid (69%) and hydrogen peroxide (35%). Subsequently, they were digested by a Microwave speedwave ENTRY (Berghof, Germany) and diluted to a final concentration of 5% of HNO_3. All samples were filtered through a 0.2 μm syringe filter and analyzed by an Agilent 7700 Series ICP-MS. Calibration standard curves of 0.1, 1, 10, 100 and 300 μg/L for all measured elements except iron were used for the quantification. For iron, a calibration standard curve of 10, 100, 1000, 10000 and 30000 μg/L was used. The calibration curves were prepared from the initial calibration verification standard (Agilent, USA): 10 ppm for arsenic, cadmium, chromium, vanadium, manganese, copper, nickel, zinc, lead and 100 ppm for iron in a matrix of 5% of nitric acid. All samples were spiked with 20 μg/L of scandium and rhodium and used as internal standards. For each sample 3 technical repetitions were performed. The Detection Limit (DL) for V, Cr, Mn, Ni, Cu, As, Cd and Pb was lower than 0.01 μg/L both in the supernatants and in the cell fractions. For Fe and Zn the DL it was lower than 0.4 μL in both phases. All samples were measured above the detection limits.

2.5. Membrane lipid peroxidation estimation

The formation of malondialdehyde (MDA) was used to evaluate membrane lipid peroxidation as a biomarker of oxidative stress. MDA derivatization was performed according to a published method developed by our group with minor modifications [19]. Briefly, after 4 h, 48 h or 72 h exposures 20 μL of cell culture medium was mixed with 25 μL of 100 ng/mL d2-MDA (internal standard solution in water) and 500 μL of 0.5 mM DNPH (in 1% formic acid solution). The mixture was kept at 37 °C and 300 rpm for 70 min in a Thermomixer C (Eppendorf, Germany). After derivatization, 700 μL of n-hexane was added and the mixture was vigorously shaken and centrifuged at 9390 rcf for 5 min in a Heraeus™ Biofuge Pico® Centrifuge (Thermo scientific, Germany). The n-hexane supernatant was transferred to a new 2 mL tube and 700 μL of fresh n-hexane was added to the mixture. Then the extraction procedure was repeated and both n-hexane supernatants were combined and dried by nitrogen in a Vapotherm basis mobil I (Barkey, Germany) at room temperature. The dried residue was re-dissolved in 50 μL of methanol:0.1% formic acid (80:20, v/v).

The MDA adduct (MDA-DNPH) was analyzed using a triple quadrupole mass spectrometer Qtrap 4000 (AB Sciex, USA) equipped with a Turbo V™ Source (Sciex, USA) enabling electrospray ionization and coupled to an HPLC system (Agilent 1290 HPLC, Agilent Technologies, USA) including a degasser, a binary pump, an autosampler, and a column compartment. The used mass spectrometer parameters were a capillary voltage of 4.5 kV, a source temperature of 350 °C, a nebulizer gas at 40 psi, heater gas 50 psi, curtain gas 20 psi, and collision gas 11 psi. The column compartment was set to 20 °C. The autosampler was set to 10 °C. The measurement was performed using multiple reaction monitoring in positive ion mode. Two transitions were selected (Table S3, supplement information). The first transition was used for quantification and the second transition was used for qualification. The separation column was a Kinetex C18 (2.6 μm, 100 Å, 100 × 3 mm i.d., Phenomenex, Germany). The mobile phase was methanol:0.1% formic acid (80:20, v/v) with a constant flow of 200 μL/min. Ten μl of each sample were injected twice into the HPLC column, and the solvent fraction eluting from 1.5 to 3.5 min from the analytical column was infused into the MS for measurement. A standard calibration curve was set up for quantification (0.4, 0.8, 2, 4, 8, 20 ng/ml). The MDA background in the blank medium without cells was subtracted from the concentration in the sample with cells and further normalized by using the respective cell number.

2.6. DNA extraction, and DNA hydrolysis

A549 and THP-1 cells were seeded and treated as described in the subsection 2.2 for 4 h and 72 h with 2 μg/mL of menadione or 3-MCPD, 200 μg/mL of CZ100 or UD 1649, or 40 μg/mL of diesel PM. DNA extraction was performed according to a salting out procedure [20]. Quantity and purity of DNA were measured spectrophotometrically (Nanodrop, Thermo Fisher, Germany). For DNA hydrolysis, 200 μg of DNA (dissolved in 400 μl of TE buffer) was mixed with 2 μl of DNA degradase plus™ according to the manufacturer's protocol and kept on an Eppendorf Thermo Mixer C with 850 rpm at 37 °C for 24 h. After DNA hydrolysis, the mixture was heated to 70 °C for 20 min to deactivate the enzyme. An aliquot of the hydrolysate was processed by solid phase extraction (using LiChrolut® EN 200MG 3 mL cartridges) and analyzed by LC-MS/MS for 8-OHdG. A second aliquot of the hydrolysate was filtered (using Acrodisc® Syringe filters) and analyzed by LC-UV for 2'-deoxyguanosine.

2.6.1. Solid phase extraction

The DNA hydrolysate (350 μL) was mixed with 50 μL of water and 100 μL of internal standard solution ($^{15}N_5$-8-OHdG, 10 ng/mL). The mixture was diluted to a total volume of 3 mL with water and the pH was adjusted to 5.0 for SPE. Firstly, 3 mL of acetonitrile, 3 mL of methanol, and 3 mL of water were used for conditioning and equilibration of the SPE cartridge. Secondly, the sample was loaded. Thirdly, 3 mL of water and 2 mL of acetonitrile were used for washing. Finally, 3 mL of methanol was applied for elution of 8-OHdG. The eluate was dried under a gentle nitrogen flow at room temperature and redissolved in 60 μL of the mobile phase (acetonitrile:water, 80:20, v/v) for LC-MS/MS analysis.

2.6.2. Determination of 8-OHdG levels

The LC-MS/MS-system used for the determination of 8-OHdG consisted of an HPLC coupled with a QTrap 4000 triple quadrupole mass spectrometer. The HPLC (Agilent 1290 HPLC, Agilent Technologies, USA) included a degasser, a binary pump, an autosampler, and a col-

umn compartment. The Qtrap 4000 was equipped with a Turbo V™ Source (Sciex, USA) enabling electrospray ionization. The following instrumental parameters were used for the mass spectrometric detection: capillary voltage, 5 kV; source temperature, 500 °C; nebulizer gas, 40 psi; heater gas, 50 psi; curtain gas, 20 psi. The measurements were carried out using multiple reaction monitoring in positive ion mode. Further parameters and the transition used are shown in Table S3. Analyst 1.6.2 software was used for instrumental control, data acquisition, and data analysis. A Eurospher II 100-3 HILIC column (3 μm, 100 Å, 100 × 3 mm i.d., Knauer, Germany) was utilized for chromatographic separation. The mobile phase consisted of a mixture of acetonitrile and water (80:20, v/v) with ammonium acetate (2 mM) at a constant flow rate of 300 μl/min. Both column oven and autosampler were set to 20 °C during analysis. The injection volume was 10 μL. Each sample was injected three times. The quantification of 8-OHdG in cells was done using a calibration curve based on relations between peak areas of the internal standard and 8-OHdG (0.16, 0.4, 1.0, 1.6, 4.0, 10, 16, 40, 100 ng/mL). For the separation and quantification of dG, an HPLC-UV system (UltiMate 3000, ThermoFisher, USA) was used. It consisted a degasser, a pump, an autosampler, a column compartment, and a UV-Vis detector. A Eurospher II 100-3 HILIC column (3 μm, 100 Å, 100 × 3 mm i.d., Knauer, Germany) was applied for the separation. The eluent was a mixture of acetonitrile and water (90:10, v/v) with ammonium acetate (20 mM) at a constant flow rate of 600 μL/min. The column oven and the autosampler were kept at 20 °C, and the detection wavelength for dG was 260 nm. The quantification of dG was performed using external calibration (dG, 0.5, 1, 2, 5, 10, 20 μg/mL).

2.7. Cytokinesis-block Micronucleus Cytome Assay

CBMN Cyt assay was performed according to Di Bucchianico et al. [21]. Briefly, A549 and THP-1 cells were seeded, as described in the subsection 2.2, 24 h prior to exposure to different compounds (2 μg/mL of menadione or 3-MCPD, 200 μg/mL of CZ100 or UD 1649, or 40 μg/mL of diesel PM). Twenty hours after exposure, a final concentration of 5 μg/mL cytochalasin-B (Sigma-Aldrich) was used to block cytokinesis. Cells were harvested after an additional 28 h culture for a total of 48 h exposure to the tested compounds. 300 μg/mL ethyl methanesulfonate (EMS) was used as positive control while 0.2 % DMSO (v/v) was used as solvent control for menadione exposures. Two slides per condition were examined in three independent experiments. The cytokinesis-block proliferation index (CBPI) indicates the average number of cell cycles during the exposure and was evaluated as a measure of cytostasis. The number of apoptotic (APO), necrotic (NEC) and mitotic (MI) cells were scored to evaluate the induced cytotoxicity. Micronuclei were evaluated in both binucleated (MN BN) and mononucleated (MN mono) cells to distinguishing between aneuploidogenic and clastogenic effects [22]. Additionally, nucleoplasmic bridges (NPB) and nuclear buds (NBUD) were also scored as biomarkers of chromosomal rearrangements and DNA repair, respectively [21].

2.8. Statistical analysis

Statistical analysis was performed using GraphPad Prism 9.1.2. One-way analysis of variance followed by multiple comparison versus control group (Dunnett´s method) was used to test the statistical significance of results expressed as mean ± standard error of mean of three independent experiments (n = 3). Pearson correlation coefficients were used for the correlation studies between MDA levels ratio, genotoxic effects and 8-OHdG persistence.

3. Results

3.1. ICP-MS elemental particles analysis

The elemental composition is available in the material certificates for few selected elements in UD 1649 and CZ100, or in Ball et al. for diesel PM [23]. Recently we published the mass fraction values of epigenetically active elements like As, Cd and Cr for the investigated reference materials [24]. For the present study, we conducted new ICP-MS analysis to evaluate the elemental concentration of V, Cr, Mn, Fe, Ni, Cu, Zn, and Pb, which could play an important role in inducing genotoxicological effects. As shown in Table 1, UD 1649 contains the highest amount of metals, notably V, As, and Pb, with respect to CZ100 which in contrast contains higher fractions of Cr, Mn, Fe and Cu. Overall the mass fraction of metals in diesel PM was low compared to the other two PM samples, however, we detected considerable amounts of Fe and Zn.

3.2. Cell viability assay

All tested compounds decreased cell viability in both epithelial A549 and monocytic THP-1 cells with increasing mass concentrations following 24 h exposure (Fig. 1). Interestingly, the oxidizers menadione and 3-MCPD caused a severe decrease of cell viability in THP-1 cells, but not in A549 cells, starting from concentrations above 2 μg/mL (Fig. 1a and b). 6 μg/mL of menadione and 8 μg/mL of 3-MCPD treatments caused a decrease of A549 cell viability to 90%. In contrast, THP-1 cell viability was reduced to 90 % with 2 μg/mL of menadione and 3-MCPD exposures. These cell-type specific effects were not observed in exposures to PM (Fig. 1c-e). The cell viability of A549 and THP-1 cells decreased to 90% when treated with 200 μg/mL of CZ100 or UD 1649 compared to 40 μg/mL of diesel PM. To avoid cytotoxic conditions and the resulting confounding effects, we chose 2 μg/mL of menadione or 3-MCPD, which gave rise to a similar extent of cytotoxicity as per 200 μg/mL of CZ100 or UD 1649, and 40 μg/mL of diesel PM in the subsequent exposure experiments.

3.3. Particle deposition analysis

UV-Vis spectrophotometric analysis of PM deposition on adherent A549 exposures was based on the detected amount of particles per surface area. In this study, 200 μg/mL of CZ100 or UD 1649, or 40 μg/mL of diesel PM were used with nominal concentrations in terms of mass per surface of 40 μg/cm^2, 40 μg/cm^2, and 8 μg/cm^2, respectively. Spectrophotometric deposition analysis revealed different deposition efficiencies among tested PM and the deposited mass were calculated as 26 ± 2 μg/cm^2, 34 ± 2 μg/cm^2, and 6 ± 0.3 μg/cm^2 for CZ100, UD 1649, and diesel PM, corresponding to a percentages of deposited parti-

Table 1
Determination of elemental concentrations (mg/kg) in the reference particles CZ100, UD 1649, and diesel PM as evaluated by ICP-MS. Data are shown as mean ± standard deviation of three measurements. *, measured in our previous study [24].

	Elements (mg/kg)		
	CZ100	UD 1649	diesel PM
Vanadium (V)	60 ± 1	349 ± 4	≈ 0.1
Chromium (Cr)*	238 ± 6	145 ± 2	≈ 4
Manganese (Mn)	586 ± 16	282 ± 2	≈ 4
Iron (Fe)	38251 ± 920	28705 ± 335	602 ± 2
Nickel (Ni)	105 ± 3	177 ± 4	≈ 3
Copper (Cu)	434 ± 12	273 ± 2	≈ 9
Zinc (Zn)	1335 ± 28	2089 ± 16	737 ± 5
Arsenic (As)*	≈ 9	78 ± 1	≈ 1
Cadmium (Cd)*	≈ 1	≈ 28	≈ 0.1
Lead (Pb)	117 ± 1	13393 ± 110	≈ 10
Total (g/Kg)	≈ 41	≈ 46	≈ 1.4

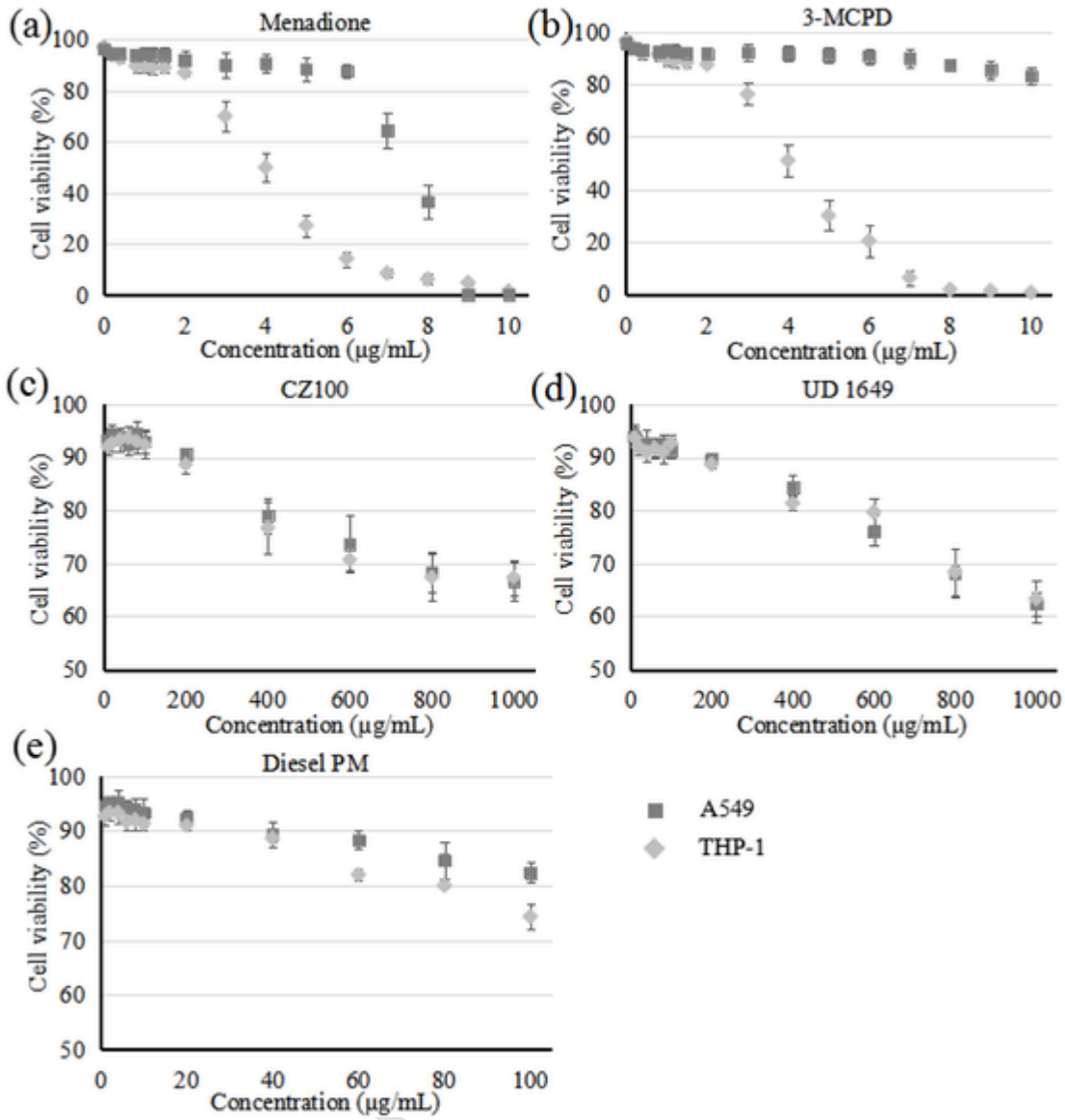

Fig. 1. Concentration-response curves for determining the concentrations of tested compounds for subsequent cell exposures. % cell viability of A549 and THP-1 cells is shown as mean ± standard error from three independent experiments following 24 h exposures to (a) menadione (b) 3-MCPD (c) fine dust CZ100 (d) urban dust UD 1649 (e) diesel PM.

cles of approximately 65 %, 85 %, and 76 %, respectively. Due to difficulties in removing particles not interacting with cells, UV-Vis spectrophotometric evaluation was not possible in suspension cultures performed with THP-1 cells.

3.4. ICP-MS ion release in cell culture medium and cellular uptake

In order to characterize the dissolution/ion release of selected elements in cell culture medium and their cellular uptake, ICP-MS analysis was conducted in both cell culture supernatants and cell pellets following 48 h exposure to 200 µg/mL of CZ100 or UD 1649, and 40 µg/mL of diesel PM, of both A549 (Fig. 2a-c) and THP-1 cells (Fig. 2d-f). A similar distribution trend for V, Cr, Mn, Fe and Ni between the supernatant and the cells was observed following both A549 and THP-1 exposure to CZ100, where these elements are mostly taken up by cells. In comparison, the cellular content of Cu, As, Cd and Pb was equal or lower with respect to the supernatant content (Fig. 2a and d). However, for CZ100 exposure a different Zn distribution between supernatants and cells was noticed in the two used cell models, and THP-1 cells showed higher Zn uptake efficacy (ca. 85%) with respect to A549 cells (ca. 30%). This clear difference could not be observed following UD 1649 exposures where approx. 46% of Zn was taken up by A549 cells and approx. 36% by THP-1 cells (Fig. 2b and e). After exposure to diesel PM, A549 cells were taking up Fe more efficiently than monocytic THP-1 while the opposite effect was observed for V and Zn (Fig. 2c and f).

The cellular associated elemental content was measured as µg/L and calculated as ng per 10^6 cells in both THP-1 (Fig. 3a) and A549 cells (Fig. 3b). The most abundant elements, which might differentiate between cell types and reference particles exposures, were Mn, Fe, Ni, Cu, Zn and Pb. However, both THP-1 and A549 cells took up considerable amount of V and Cr following exposures to CZ100 or UD 1649. No differences on Mn uptake were observed between the cell types and the higher cellular content of Mn after CZ100 treatments was in line with the higher Mn content of CZ100 particle compared to that of UD 1649. Interestingly this coherency was not observed for Fe uptake, since no clear differences on iron cellular content could be shown after CZ100 or UD 1649 exposures despite the diverse particles content of Fe. This was especially the case in monocytic THP-1 exposure. Furthermore, the cellular Fe content was ten times higher, ca. 0.7 ng/10^6 cells, following A549 exposure to Diesel PM compared to THP-1 treatments. Clear dif-

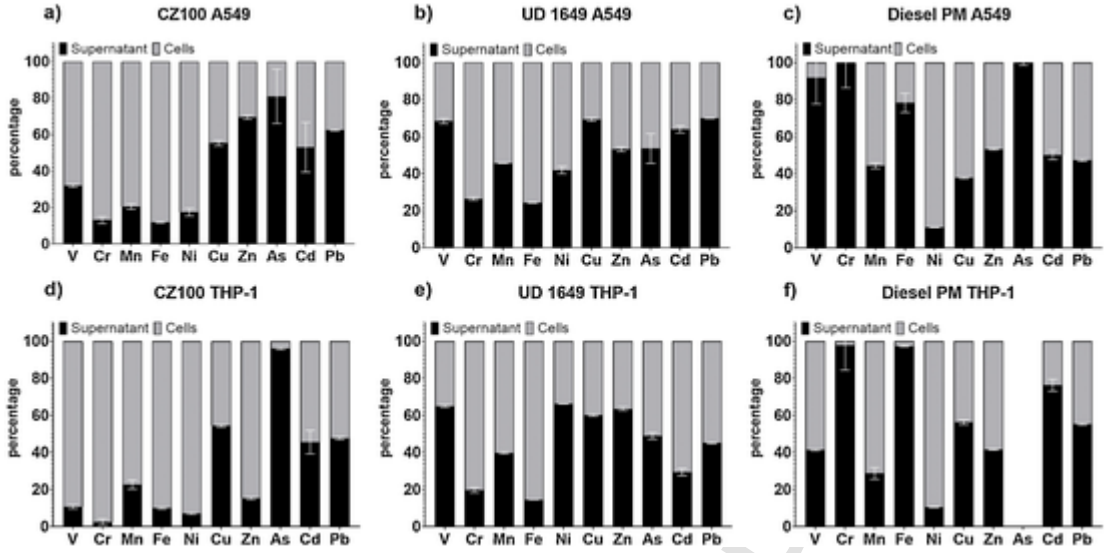

Fig. 2. The amount of selected elements was analyzed by ICP-MS following 48 h exposure of A549 cells to CZ100 (a), UD 1649 (b), Diesel PM (c), and THP-1 cells to CZ100 (d), UD 1649 (e), and Diesel PM (f). Data are expressed as mean % distribution of elements in supernatant (black) and cells (gray) ± SD.

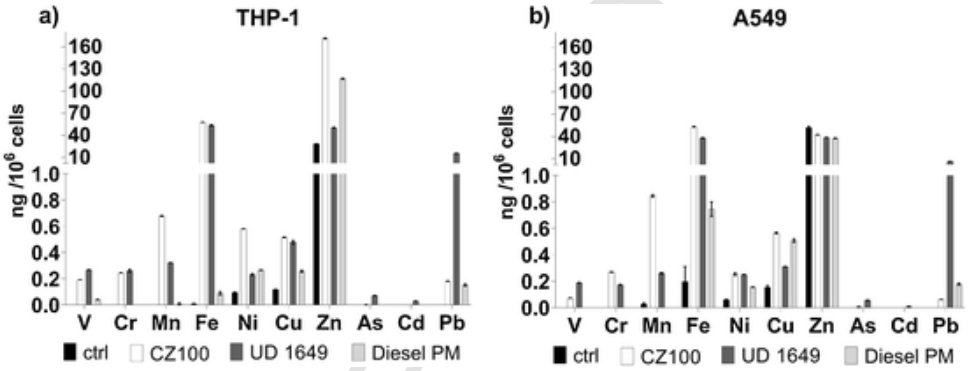

Fig. 3. Cellular content of selected elements was analyzed by ICP-MS following 48 h exposure of THP-1 (a) and A549 cells (b) to CZ100, UD 1649, or Diesel PM. Data are expressed as mean ± SD.

ferences between cell types as well as among reference particle treatments could be seen for Zn cellular content. Untreated A549 cells contained a larger amount of Zn compared to monocytic THP-1, ca. 52 ng/10^6 A549 cells versus ca. 28 ng/10^6 THP-1 cells. Following exposures to PM, the cellular content of Zn was decreasing in A549 cells regardless of the particle types and their relative Zn content, while after THP-1 exposures to PM, up to 6-fold and 4-fold increase of Zn uptake was observed for CZ100 and Diesel PM treatments, respectively, regardless the relative Zn particles content. As expected, Pb uptake significantly increased following exposure to UD 1649 due to the significantly higher Pb content of these reference particles. However, considerable cellular content of Pb was observed following CZ100 and Diesel PM exposures.

3.5. CZ100 is more effective in inducing lipid peroxidation

To assess oxidative stress induced by PM and oxidizers we evaluated MDA levels following 4, 48, and 72 h exposures (Fig. 4). The fine dust CZ100 particles significantly increased MDA levels with a decreasing trend from 4 h to 72 h exposure in THP-1 cells while the oxidizer 3-MCPD showed a significant MDA release only after the shorter exposure time (Fig. 4a). A slight increase of MDA level was observed following 4 h exposure of THP-1 cells to Diesel PM (Fig. 4a). Following A549 treatments with CZ100 the released amount of MDA was approximately doubled and similar over the exposure times, but a statistical significant increase was only observed following 4 h treatment (Fig. 4b). A slight increase of MDA was noticed after both 4 h and 72 h exposures of A549 to UD 1649. The oxidizer 3-MCPD induced a significant MDA release on 4 h treated A549 to a similar extent found for THP-1 while menadione was inducing a double amount of MDA production with respect to untreated A549 without statistical significance (Fig. 4b).

3.6. Reference PM induce persistent 8-OHdG lesions

The basal amount of oxidative 8-OHdG lesions in both THP-1 and A549 cells equaled approximately five lesions per 10^6 nucleobases (Fig. 5). Representative mass spectra for the analysis of 8-OHdG is shown in Fig. S1. Elevated oxidative stress levels were accompanied by an increase in the levels of 8-OHdG lesions in both THP-1 (Fig. 5a) and A549 cells (Fig. 5b) following both short and long exposure times, indicating a persistent DNA oxidation. In THP-1 cells both reference particles and oxidizers induced significant DNA oxidation in a similar extent, but differences were observed in terms of DNA oxidation persistence measured as the ratio between the effects detected following 72 h and 4 h exposures. In fact, DNA oxidation induced by CZ100 decreased by 3.3 fold during time with a ratio of 0.33, similar to the 3.8 fold decrease observed upon menadione treatments (ratio of 0.39). The effects induced by UD 1649 and diesel PM decreased by 4.7 and 4.9 fold, with a ratio of 0.22 and 0.24 respectively, indicating a lower persistency of DNA oxidation with respect to both CZ100 and menadione treatments (Table 2). All exposures induced significant DNA oxidation in A549 cells after both 4 h and 72 h exposures (Fig. 5b) whereas diesel PM was more ef-

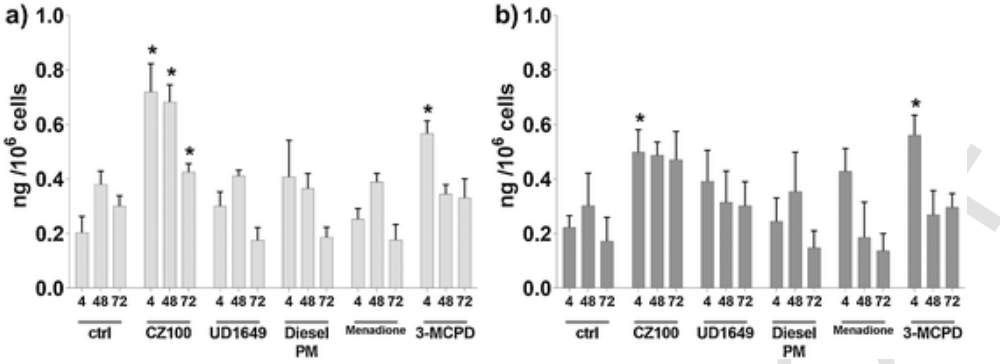

Fig. 4. MDA levels expressed as ng per million of cells in monocytic THP-1 cells (a) and A549 (b) following 4 h, 48 h and 72 h exposures to 200 μg/mL of CZ100 or UD 1649, or 40 μg/mL of diesel PM, or 2 μg/mL of menadione or 3-MCPD. Data are shown as mean ± standard error from three independent experiments. * = *p*-value < 0.05 compared to the relative untreated control (ctrl).

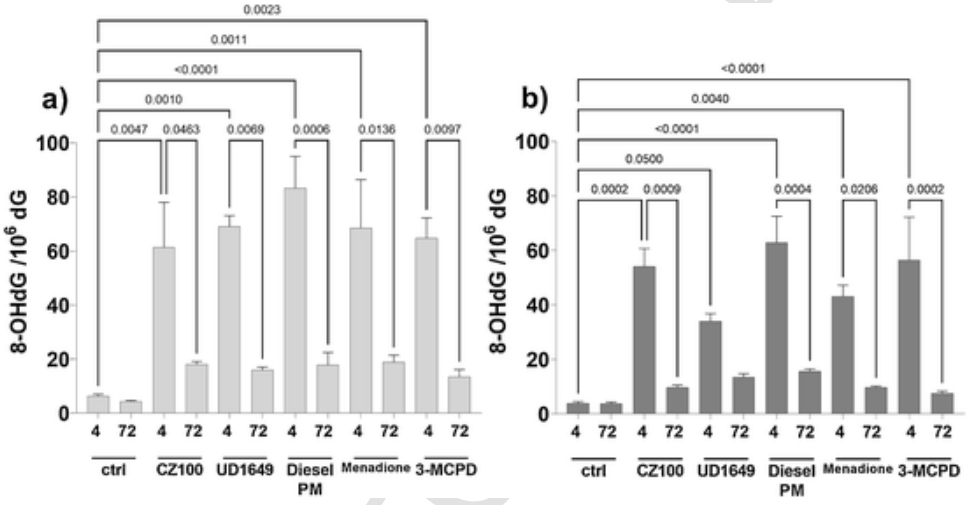

Fig. 5. 8-OHdG levels in THP-1 (a) and A549 (b) cells unexposed (ctrl) and exposed for 4 h or 72 h to 200 μg/mL of CZ100 or UD 1649, or 40 μg/mL of diesel PM, or 2 μg/mL of menadione or 3-MCPD,. Results are shown as mean ± standard error of three independent experiments and p-values indicate statistical significance differences.

Table 2
Mean values (± standard error) of 8-OHdG persistency in THP-1 and A549 cells exposed to different substance calculated as the ratio between the effects observed following 72 h and 4 h treatments.

Cells	Ctrl	Particles			Oxidizers	
		CZ100	UD 1649	Diesel PM	Menadione	3-MCPD
THP-1	0.79 ± 0.25	0.33 ± 0.07	0.22 ± 0.03	0.24 ± 0.06	0.39 ± 0.12	0.21 ± 0.03
A549	1.0 ± 0.1	0.22 ± 0.07	0.42 ± 0.10	0.29 ± 0.08	0.23 ± 0.03	0.18 ± 0.07

fective than UD 1649 and the oxidizer menadione after the shorter exposure time. Also following 72 h exposure diesel PM treatments were more effective than CZ100 and the two oxidizers in inducing DNA oxidation. However, the effects induced by UD 1649 were more persistent over the exposure time as indicated by a 2.6 fold changes between 4 h and 72 h exposures corresponding to a ratio of 0.42 (Table 2). In general, considering the lower exposure concentration and deposition, diesel PM showed the highest DNA oxidative capacity with respect to both UD 1649 and CZ100. After treatments, THP-1 cells generally showed higher DNA oxidation levels compared to those of A549 cells.

3.7. CBMN cyt assay

A representative distribution of mononucleated, binucleated, and polynucleated cells used to calculate the CBPI is shown in Fig. 6a while a typical mitotic cell used to evaluate the mitotic index is shown in Fig. 6b. Apoptotic and necrotic cells are shown in Fig. 6c and 6d, respectively, and were used to assess the cytotoxic potential of oxidizers and PM. Micronuclei formation in both mononucleated (Fig. 6e) and binucleated cells (Fig. 6f) was analyzed as a hallmark of aneuploidogenic and clastogenic effects, respectively [22,25]. Nucleoplasmic bridges (Fig. 6g) as well as nuclear buds (Fig. 6h) were scored as biomarkers of chromosome rearrangements or telomere end-fusion and as biomarker of amplified DNA elimination, respectively [21].

Besides menadione, which reduced cell proliferation in THP-1 cells, none of the tested compounds showed anti-proliferative effects (Fig. 7a). While all PM samples and oxidizers significantly reduced the mitotic index in THP-1 cells from 4.8 % in control cells to approximately 3 % (Fig. 7b), only minor cytotoxic changes in terms of apoptotic and necrotic effects were noticed (Fig. 7c and 7d).

In terms of genotoxic potential, a significant induction of MN in mono- and binucleated cells was observed in A549 exposed to diesel PM and oxidizers (Fig. 8a and 8b). Only after exposure to menadione a significant increase of MN in binucleated cells was observed in THP-1 cells

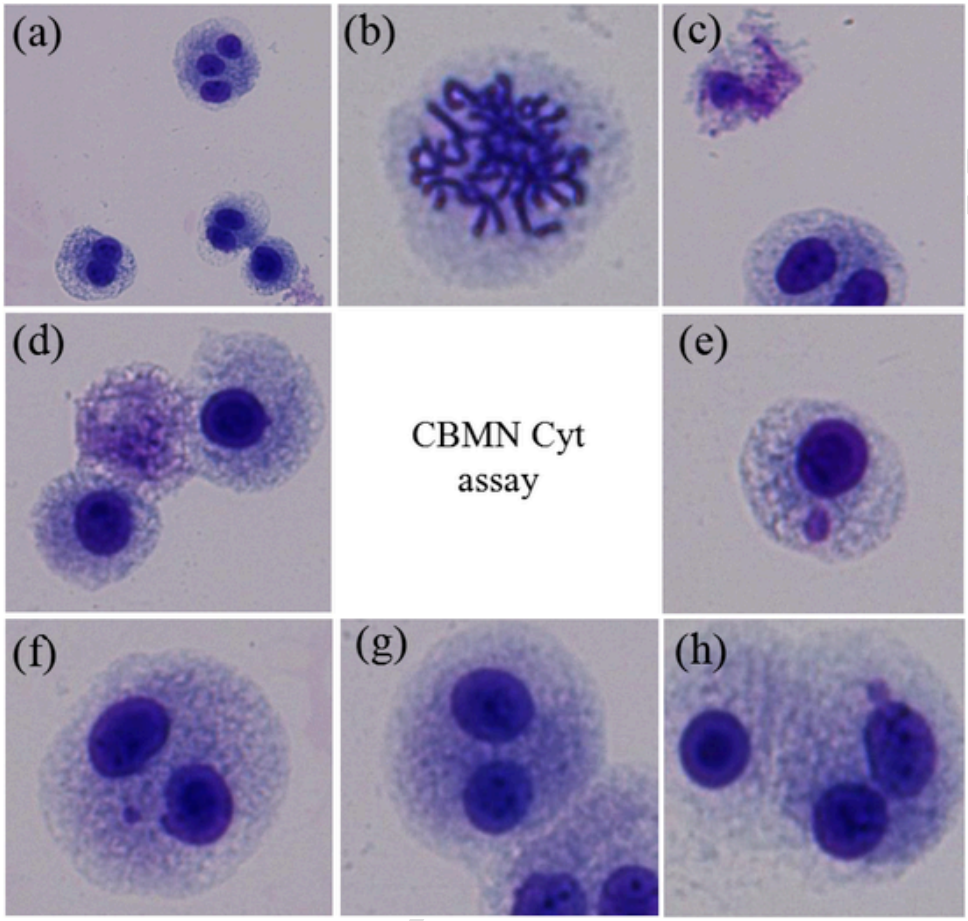

Fig. 6. (a) Exemplary distribution of mononucleated, binucleated and polynucleated THP-1 cells (b) mitotic cell (c) apoptotic cell (d) necrotic cell used to assess cytostasis and cytotoxicity by CBMN Cyt assay (e) micronucleus in mononucleated THP-1 cell (f) micronucleus in binucleated THP-1 cell (g) nucleoplasmic bridge (NPB) (h) and nuclear bud (NBUD) were evaluated in order to comprehensively detect induced genotoxic mechanisms.

(Fig. 7b). In contrast, a significant induction of NPB formation occurred in both cell types following exposure to CZ100 and oxidizers (Fig. 8c). Diesel PM exposure significantly induced NPB formation on A549 cells. On the other hand, NBUD slightly increased in both THP-1 and A549 cells (Fig. 8d). Generally, diesel PM and oxidizers were more effective in inducing chromosomal damage compared to CZ100 and UD 1649 particles.

3.8. Correlations between 8-OHdG persistency, chromosomal instability and oxidative stress

8-OHdG persistence was evaluated based on the ratio between 72 h and 4 h exposures of 8-OHdG/10^6 dG values (Table 2) in order to depict possible correlations among 8-OHdG formation dynamics and the genotoxic biomarkers as well as with MDA levels ratio between 72 h and 4 h exposures. Pearson correlation data are shown for CZ100, diesel PM, menadione and 3-MCPD treatments on A549 (Fig. 9a, 9b. 9c. 9d) and THP-1 cells (Fig. 9e, 9f, 9 g, 9 h). Correlations following exposure to UD 1649 were due to the lack of significantly increased chromosomal instability and therefore considered as not relevant and are not displayed. There was a significant positive correlation between 8-OHdG persistence and MN in binucleated cells (MN BN) following A549 exposures to diesel PM (R^2 = 0.998, p = 0.021; Fig. 9b) and the oxidizer 3-MCPD (R^2 = 0.984, p = 0.05; Fig. 9d). A strong positive correlation was observed between the DNA oxidation persistency and NPB formation after A549 exposures to diesel PM (R^2 = 1.0, p = 0.001; Fig. 9b) and to 3-MCPD (R^2 = 0.988, p = 0.05; Fig. 9d), as well as after THP-1 treatments with diesel PM (R^2 = 1.0, p = 0.005; Fig. 9f) and menadione (R^2 = 1.0, p = 0.017; Fig. 9g). We also observed that the induction of NPB had a strong positive correlation with MN induction in binucleated A549 cells after exposure to CZ100 (R^2 = 1.0, p = 0.018; Fig. 9a), diesel PM (R^2 = 0.998, p = 0.021; Fig. 9b), and the oxidizer 3-MCPD (R^2 = 1.0, p = 0.009; Fig. 9d). The lipid peroxidation biomarker MDA was positively correlated with MN BN after A549 treatments with CZ100 (R^2 = 0.994, p = 0.05; Fig. 9a) and menadione (R^2 = 1.0, p = 0.017; Fig. 9c), and negatively correlated with MN mono in A549 cells following 3-MCPD treatment (R^2 = 1.0, p = 0.013; Fig. 9d).

4. Discussion

Recently we showed that the content of metals and PAHs of reference particulate matter differently shapes epigenetic DNA modifications on monocytic THP-1 cells and that CZ100 was more effective than UD 1649, diesel SRM2975, and the oxidizer tert-butyl hydroxiperoxide in inducing cytosine demethylation, cytosine hydroxymethylation, and adenine methylation [24]. CZ100 is characterized by a similar distribution of PAHs with respect to UD 1649, but with a lower amount of toxic compounds such as benzo(a)pyrene and benzo(a)anthracene among others (Table S1). CZ100 is also the applied PM with the highest content of metals with a total elemental content 3.4 times higher than UD 1649 as reported in the respective material certificates, and particularly rich in Cr, Mn, Fe, and Cu as confirmed by the present study (Table 1 and S2). On the other hand, UD 1649 is particularly abundant in toxic elements like V, Ni, Zn, As, Cd and Pb, while having a lower total metal content compared to CZ100. Diesel PM is characterized by a lower amount of PAHs compared to CZ100 and UD 1649, but it contains

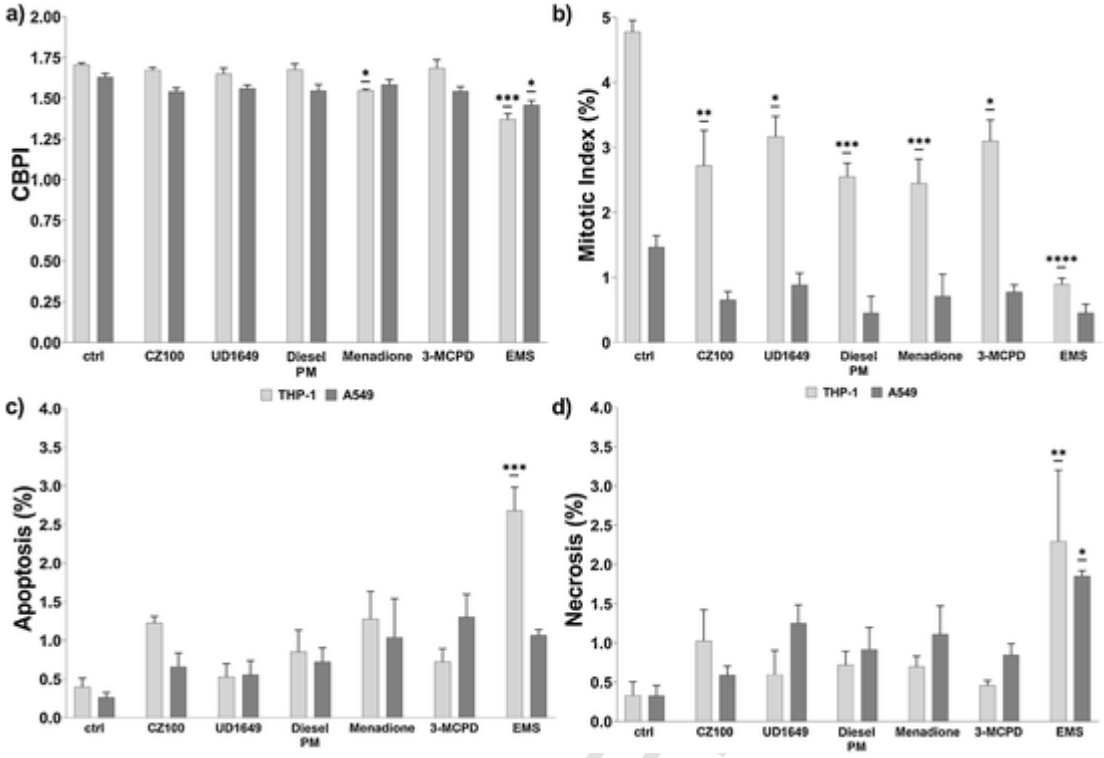

Fig. 7. CBMN Cyt assay, cytostasis and cytotoxicity. The cytokinesis-block proliferation index (CBPI, a), the % of mitotic (b), apoptotic (c) and necrotic cells (d) are presented as mean ± standard error from three independent experiments (2 μg/mL of menadione or 3-MCPD, 200 μg/mL of CZ100 or UD 1649, or 40 μg/mL of Diesel PM). *, $p < 0.05$; **, $p < 0.01$; ***, $p < 0.001$. Underlined asterisks denote statistical significance for both cell types with respect to their relative controls.

larger amount of nitro-PAHs, e.g. the high toxic 1,6-dinitropyrene, and considerable amounts of Zn and Fe (Table 1 and S1). Despite the different metal content of the particles, we have shown that the ion release into cell culture media can vary among particle types as well as among cell model systems. For instance, this behavior was translated into a similar Fe cellular uptake in epithelial A549 cells following CZ100 and UD 1649 exposures despite the particle iron content, which is 1.4 times higher in CZ100 compared to UD 1649. Furthermore, even though UD 1649 contained the highest amount of Zn, the cellular content of Zn in monocytic THP-1 was much higher following exposures to CZ100 and diesel PM compared to the Zn content after exposure to UD 1649. Such observations call for more in-depth studies on physico-chemical, structural, and electronic properties of PM that can regulate metal bioaccessibility. Recently, the importance of bioaccessible metal fractions versus the total metal content was highlighted as an important aspect for calculating the carcinogenic and non-carcinogenic risk indexes of several airborne PM sources, demonstrating that health risks can be accurately predicted by the fraction of bioaccessible metals rather than the total metal content [26]. However, the variety of inorganic and organic compounds of PM samples could be specifically responsible for different PM-induced genotoxic mechanisms of action. For instance, transition metals can induce intracellular ROS via Fenton-like reactions while the metabolization of PAHs can produce reactive intermediates able to undergo redox cycling mechanisms, which are subsequently responsible for oxidative stress conditions, or generating highly reactive molecules that are directly reacting with biomolecules including DNA. One source of weakness in the present study is that only one exposure concentration per item was used, thus hiding the possibility to observe different mechanisms of action and effects. However, we focused on the time course of different toxicological endpoints to possibly highlight the role of oxidative stress and DNA oxidation persistence in inducing chromosomal instability.

In the present study we have shown that CZ100 and the oxidizer 3-MCPD significantly induced lipid peroxidation in both cell types with 4 h exposure more effective than 72 h, while all other tested materials slightly increased MDA levels following the shorter exposure time. Neutral aqueous extracts of UD 1649 and diesel SRM2975 were previously used to evaluate ROS induction via the formation of MDA from 2-deoxyribose [23]. This study showed that UD 1649 was more effective than diesel SRM2975 in generating MDA and that this effect was inhibited by the chelating agent deferoxamine, therefore suggesting that transition metals are catalyzing the formation of ROS [23]. Accordingly, lipid peroxidation observed in our study might be explained by the higher metal content of CZ100 and the subsequent higher elemental cellular uptake observed in both cell types. However, the efficacy of CZ100 in inducing lipid peroxidation, as well as its more pronounced effects with respect to UD 1649 and diesel PM treatments, was more evident in monocytic THP-1 compared to alveolar epithelial A549 cells. Recently, further research has shown that organic extracts from airborne PM reduce lipid peroxidation, as evaluated by 15-F2t-Isoprostane, via aryl hydrocarbon receptor inhibition of prostaglandin endoperoxide synthase 2 expression in A549 cells. This effect was not observed in normal human embryonic lung fibroblasts HEL12469, suggesting that processes related to lipid peroxidation are highly specific for different cell lines [27,28]. These observations also suggest a complex interplay between metal and organic particle content induced effects and their pro-oxidant potential. For instance, the observed 8-OHdG formation could not be exclusively attributed to the particles metal content since Diesel PM was the most effective in inducing DNA oxidation in both cell types. Indeed, we have shown that all tested reference particles and oxidizers promoted the generation of 8-OHdG in both monocytic THP-1 and epithelial A549 cells with a DNA oxidation persistence varying among particles and cell types in sub-cytotoxic conditions.

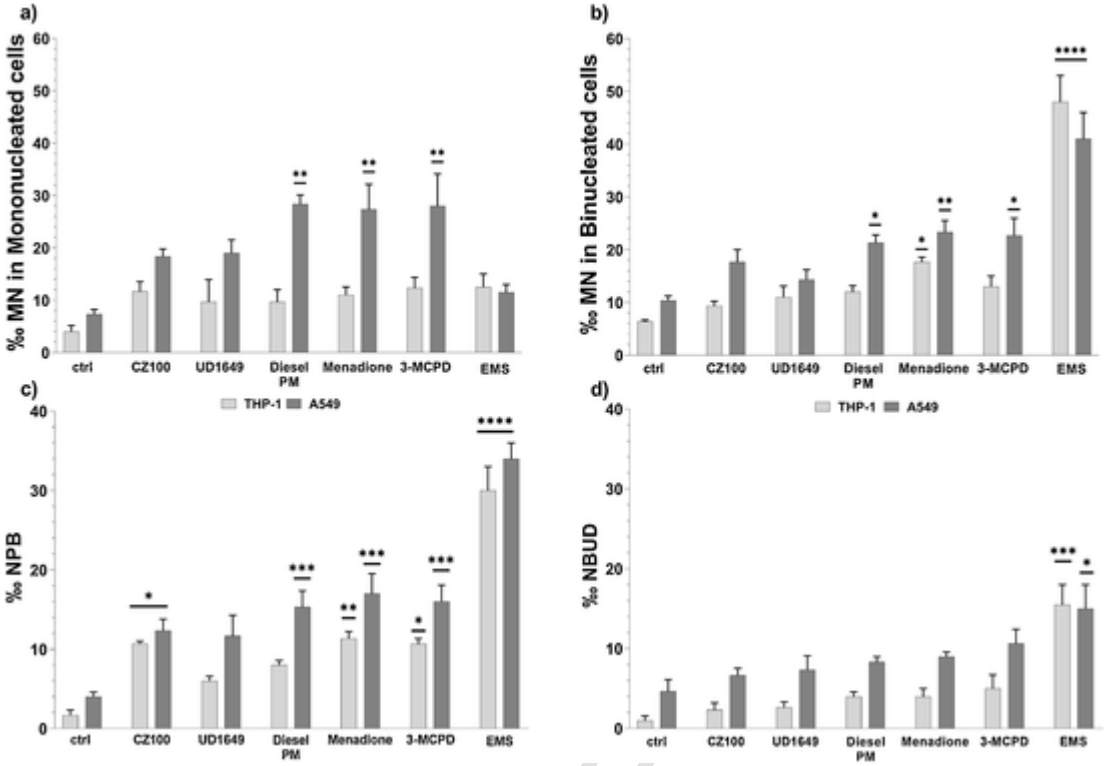

Fig. 8. CBMN Cyt assay, chromosomal damage and rearrangements. Micronuclei in mononucleated cells (a) and in binucleated cells (b), nucleoplasmic bridges (c) and nuclear buds (d) frequencies are presented as mean ± SEM from three independent experiments (2 μg/mL of menadione or 3-MCPD, 200 μg/mL of CZ100 or UD 1649, or 40 μg/mL of diesel PM). 300 μg/mL ethyl methanesulfonate (EMS) was used as positive control. *, $p < 0.05$; **, $p < 0.01$; ***, $p < 0.001$, ****, $p < 0.0001$ with respect to the relative controls (ctrl).

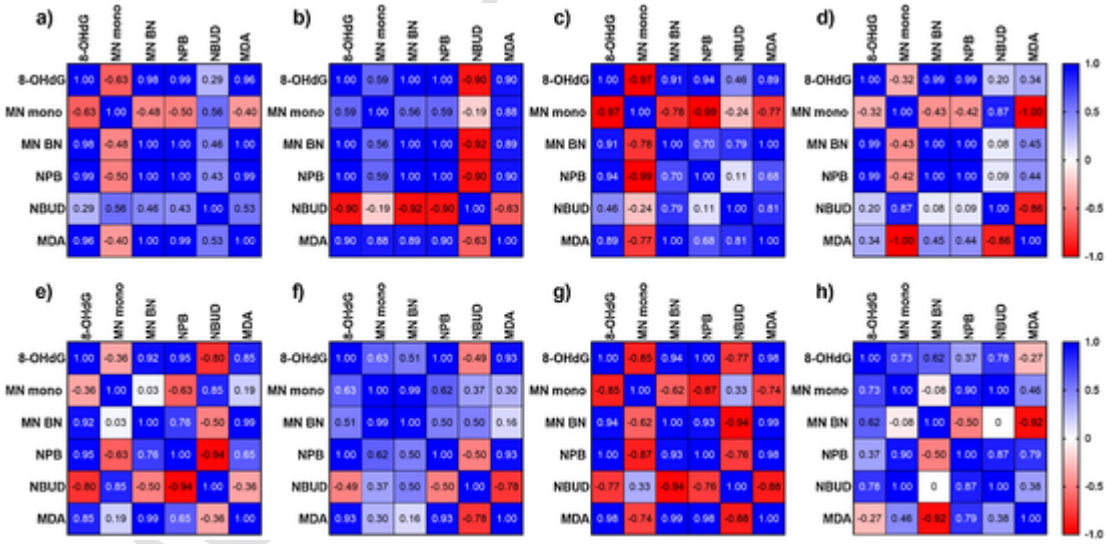

Fig. 9. Pearson´s correlation coefficients of 8-OHdG persistency (ratio between 72 h and 4 h effects), MN in mononucleated cells (MN mono), MN in binucleated cells (MN BN), nucleoplasmic bridges (NPB), nuclear buds (NBUD), and the ratio of malondialdehyde (MDA) production between 72 h and 4 h exposures of A549 to CZ100 (a), diesel PM (b), menadione (c), 3-MCPD (d), and following monocytic THP-1 exposures to CZ100 (e), diesel PM (f), menadione (g), and 3-MCPD (f).

The organic content of PM samples and its pro-oxidant activity could also constitute a driving factor for DNA oxidation and chromosomal instability. For instance, we observed a significant induction of MN in A549 cells after exposure to diesel PM and both tested oxidizers (menadione and 3-MCPD) which were positively correlated with 8-OHdG lesions persistency. Moreover, in both cell lines, we found significantly increased NPB formation after CZ100 and oxidizer treatments, which were positively associated with NPB but not with NBUD.. NPB formation was positively correlated with 8-OHdG persistence in both cell types, with a significant correlation following diesel PM and oxidizers. NPB originating from dicentric chromosomes and centric ring chromosomes are a sensitive measure of chromosomal damage induced by ROS, and positive correlations of NPB with MN and NBUD were shown in previous studies on oxidative stress and genotoxicity in human lymphoblastoid WIL2-NS cell line [29,30]. However, we found conflicting correlations between NPB and NBUD with varying treatments and cell type, and no significant increase of NBUD was noticed.

In particular for UD 1649 treatments, the increase of 8-OHdG levels in THP-1 cells was higher than in A549, in terms of absolute frequencies, asking for a better understanding of the role of cell-specific metabolism with regards to the different PAHs and metal content of tested particles. In fact, besides CZ100, which showed a similar DNA oxidation capacity between the two distinct cell models, UD 1649 induced DNA oxidation was more persistent in A549 than monocytic THP-1 cells. Prahalad et al. reported that the level of 8-OHdG in bronchial BEAS-2B cells treated for 2 h with urban dust particles (UD 1649) increased 1.7-fold compared to untreated controls [31]. However, the oxidative capacity of UD 1649 could not be attributed to the total metal content but to its water-soluble fraction since both metal ion chelators and hydroxyl radical scavenger particle pretreatments were ineffective in inhibiting the induced DNA hydroxylation in cell-free systems [31]. Similarly, diesel SRM2975 generated oxidative DNA damage in A549 cells in a dose-dependent manner but was not able to induce 8-oxodG in calf thymus DNA even following co-exposure with H_2O_2, indicating the lack of metal-catalyzed reactions in the solvent because of low levels of transition metals in SRM2975 [32].

Coherently, in the current study all PM samples increased 8-OHdG levels in both cell types, which could be explained by their PAHs and nitro-PAHs content due to the low amount of metals in diesel SRM2975 and its slightly higher effectiveness in inducing DNA oxidation. This assumption is supported by the role played by CYP1A1 enzymes, mainly responsible for metabolization or oxidation of PAHs, as previously shown in murine embryonic fibroblasts and alveolar macrophages, where UD 1649 and diesel SRM2975 caused an increased CYP1A1 expression [33,34]. Moreover, Shi and co-authors investigated diesel SRM2975 induced chromosomal damage mechanisms on V79 fibroblasts and found that the particle organic solvent extracts significantly increased MN frequency, while no effects were observed after particle washing [35]. This indicates that the genotoxicity of diesel SRM2975 can be attributed to its organic components PAHs and nitro-PAHs. Specifically, nitro-PAHs are more toxic than PAHs [36]. For instance, by comparing the cytoxicity of benzo[a]pyrene, 1-nitropyrene, and 3-nitrofluoranthene it was shown that both nitro-PAHs induced higher cytotoxicity than benzo[a]pyrene [37]. One of the most abundant nitro-PAHs in diesel SRM2975, 1-nitropyrene, induced strong DNA damage and oxidative stress *in vivo,* and greatly promoted inflammation, apoptosis and necrosis in human bronchial epithelial BEAS-2B cells *in vitro* [38,39]. A direct comparison of PAHs and nitro-PAHs was conducted on BEAS-2B cells showing that 1-nitropyrene and 3-nitrobenzanthrone were more effective than benzo(a)pyrene in inducing micronuclei formation [40]. Furthermore, 1-nitropyrene and 3-nitrofluoranthene were shown to be genotoxic and cause ROS generation and inflammatory processes by activating PI3K/Akt signaling in A549 cells [41,42].

Chromosomal instability can results from persistent DNA oxidation since the simultaneous removal of multiple 8-OHdG can cause DNA double-strand breaks leading to MN formation [43]. It is important to note that persistent activation of DNA damage-related signaling was found in response to complex mixtures of air PM extract fractions containing PAHs with more than four aromatic rings but without polar compounds [44]. However, the relative PAHs composition of PM is not conserved in the atmosphere but is subjected to dynamic atmospheric aging processes, which in turn induce changes on the bioaccessibility of PAHs. Whereas UD 1649 particles could be affected mainly by the photo-oxidation reactions during daytime, CZ100 could be a result of accumulation of nitro-PAHs by diesel engine emissions and the fresh formation of nitro-PAHs, since mainly dark reactions are taking place in a tunnel and the exclusion of ozone and UV light prevents fast degradation of nitro-PAH. For instance, precursor PAH can react with nitrate radicals and further with NO_2 to form nitro-PAH [36]. The atmospheric ageing of particles collected for UD 1649 surely included similar dark reactions during nighttime but photo-oxidation during daytime can lead to both the formation and the decay of nitro-PAH. The formation of nitro-PAH is due to reaction with hydroxyl radicals and subsequent reaction with NO_2 [45]. However, a concurrent pathway of precursor PAH leads to the formation of oxygenated PAH by reaction with ozone or hydroxyl radicals which are responsible for the decay reactions [46] possibly explaining the lower genotoxic potential of UD 1649 with respect to CZ100 and diesel PM.

5. Conclusions

In this study, we investigated the oxidative capacity and persistency of reference PM fine dust CZ100, urban dust UD 1649, and Diesel PM compared to the oxidizers menadione, and 3-MCPD on epithelial A549 and monocytic THP-1 cells. Despite differences in PM tested concentrations and cellular metal uptake, all reference PM samples induced oxidative DNA damage in a comparable magnitude of order compared to the two tested oxidizers but with different persistence. Diesel SRM2975 are more genotoxic compared to fine and urban dust highlighting the role of PAH derivatives on chromosomal instability. Furthermore, we explored the correlation between 8-OHdG lesion persistency and biomarkers of chromosomal damage showing that the NPB measure is a sensitive indicator of genotoxicity induced by airborne particles and oxidative stress, and that a connection between DNA oxidation and chromosomal instability is associated with PM exposure. Additionally, a complex interplay between bioaccessible metals and PAHs particle content was shown pointing out the importance of PAH derivatives in driving reference airborne particle induced genotoxicity. Further studies are needed to explore the role of concentration-response dependent mechanisms of action of tested items.

Data Availability

We have reviewed published papers, most of which have not yet made their raw EEG data available.

Data will be made available on request.

Funding

The Helmholtz Virtual Institute of Complex Molecular Systems in Environmental Health (HICE) via the Helmholtz Association of German Research Centers (HFG), the aeroHEALTH Helmholtz International Lab., and the China Scholarship Council funded this work.

Declaration of Competing Interest

The authors report no declarations of interest.

Appendix A. Supplementary data

Supplementary material related to this article can be found, in the online version, at doi:https://doi.org/10.1016/j.mrgentox.2022.503446.

References

[1] F. Liu, G. Chen, W. Huo, C. Wang, S. Liu, N. Li, S. Mao, Y. Hou, Y. Lu, H. Xiang, Associations between long-term exposure to ambient air pollution and risk of type 2 diabetes mellitus: A systematic review and meta-analysis, Environ. Pollut. 252 (2019) 1235–1245, https://doi.org/10.1016/j.envpol.2019.06.033.

[2] R.B. Hayes, C. Lim, Y. Zhang, K. Cromar, Y. Shao, H.R. Reynolds, D.T. Silverman, R.R. Jones, Y. Park, M. Jerrett, J. Ahn, G.D. Thurston, PM2.5 air pollution and cause-specific cardiovascular disease mortality, Int. J. Epidemiol. (2019) 1–11, https://doi.org/10.1093/ije/dyz114.

[3] N. Wang, K. Mengersen, M. Kimlin, M. Zhou, S. Tong, L. Fang, B. Wang, W. Hu, Lung cancer and particulate pollution: A critical review of spatial and temporal analysis evidence, Environ. Res. 164 (2018) 585–596, https://doi.org/10.1016/j.envres.2018.03.034.

[4] L. Risom, P. Møller, S. Loft, Oxidative stress-induced DNA damage by particulate air pollution, Mutat. Res., Fundam. Mol. Mech. Mutagen. 592 (2005) 119–137, https://doi.org/10.1016/j.mrfmmm.2005.06.012.

[5] Y. Wang, J. Lin, J. Shu, H. Li, Z. Ren, Oxidative damage and DNA damage in lungs of an ovalbumin-induced asthmatic murine model, J. Thorac. Dis. 10 (2018) 4819–4830, https://doi.org/10.21037/jtd.2018.07.74.
[6] T.J. Grahame, R.B. Schlesinger, Oxidative stress-induced telomeric erosion as a mechanism underlying airborne particulate matter-related cardiovascular disease, Part. Fibre Toxicol. 9 (2012) 21, https://doi.org/10.1186/1743-8977-9-21.
[7] N. Li, T. Xia, A.E. Nei, The role of oxidative stress in ambient particulate matter-induced lung diseases and its implications in the toxicity of engineered nanoparticles, Free Radicals Biol. Med. 44 (2008) 1689–1699, https://doi.org/10.1016/j.freeradbiomed.2008.01.028.
[8] K. Donaldson, L. Tran, L.A. Jimenez, R. Duffin, D.E. Newby, N. Mills, W. MacNee, V. Stone, Combustion-derived nanoparticles: a review of their toxicology following inhalation exposure, Part. Fibre Toxicol. 2 (2005) 10, https://doi.org/10.1186/1743-8977-2-10.
[9] H.L. Karlsson, J. Nygren, L. Möller, Genotoxicity of airborne particulate matter: the role of cell-particle interaction and of substances with adduct-forming and oxidizing capacity, Mutat. Res., Genet. Toxicol. Environ. Mutagen. 565 (2004) 1–10, https://doi.org/10.1016/j.mrgentox.2004.07.015.
[10] I. Abbas, G. Garçon, F. Saint-Georges, V. Andre, P. Gosset, S. Billet, J. Le Goff, A. Verdin, P. Mulliez, F. Sichel, P. Shirali, Polycyclic aromatic hydrocarbons within airborne particulate matter (PM2.5) produced DNA bulky stable adducts in a human lung cell coculture model, J. Appl. Toxicol. 33 (2013) 109–119, https://doi.org/10.1002/jat.1722.
[11] G. Çakmak, P. Ertürk Arı, E. Emerce, A. Arı, M. Odabaşı, R. Schins, S. Burgaz, E.O. Gaga, Investigation of spatial and temporal variation of particulate matter in vitro genotoxicity and cytotoxicity in relation to the elemental composition, Mutat. Res., Genet. Toxicol. Environ. Mutagen. 842 (2019) 22–34, https://doi.org/10.1016/j.mrgentox.2019.01.009.
[12] W.J. Cannan, D.S. Pederson, Mechanisms and Consequences of Double-Strand DNA Break Formation in Chromatin, J. Cell. Physiol. 231 (2016) 3–14, https://doi.org/10.1002/jcp.25048.
[13] N. Chatterjee, G.C. Walker, Mechanisms of DNA damage, repair, and mutagenesis, Environ. Mol. Mutagen, Environ. Mol. Mutagen. 58 (2017) 235–263, https://doi.org/10.1002/em.22087.
[14] P. Pfeiffer, W. Goedecke, G. Obe, Mechanisms of DNA double-strand break repair and their potential to induce chromosomal aberrations, Mutagenesis. 15 (2000) 289–302, https://doi.org/10.1093/mutage/15.4.289.
[15] A. Murphy, A. Casey, G. Byrne, G. Chambers, O. Howe O, Silver nanoparticles induce pro-inflammatory gene expression and inflammasome activation in human monocytes, J Appl Toxicol. 36 (2016) 1311–1320, https://doi.org/10.1002/jat.3315.
[16] D.N. Criddle, S. Gillies, H.K. Baumgartner-Wilson, M. Jaffar, E.C. Chinje, S. Passmore, M. Chvanov, S. Barrow, O.V. Gerasimenko, A.V. Tepikin, R. Sutton, O.H. Petersen, Menadione-induced reactive oxygen species generation via redox cycling promotes apoptosis of murine pancreatic acinar cells, J. Biol. Chem. 281 (2006) 40485–40492, https://doi.org/10.1074/jbc.M607704200.
[17] X. Sun, L. Zhang, H. Zhang, H. Qian, J. Ji, L. Tang, Z. Li, G. Zhang, Electrochemical detection of 8-hydroxy-2'-deoxyguanosine as a biomarker for oxidative DNA damage in HEK293 cells exposed to 3-chloro-1,2-propanediol, Anal. Methods. 7 (2015) 6664–6671, https://doi.org/10.1039/c5ay01246e.
[18] C.J. Rudd, K.A. Stromt, A spectrophotomeric method for the quantitation of Diesel Exhaust Particles in Guinea Pig Lung, J. Appl. Toxicol. 1 (1981) 83–87, https://doi.org/10.1002/jat.2550010207.
[19] X. Wu, J. Lintelmann, S. Klingbeil, J. Li, H. Wang, E. Kuhn, S. Ritter, R. Zimmermann, Determination of air pollution-related biomarkers of exposure in urine of travellers between Germany and China using liquid chromatographic and liquid chromatographic-mass spectrometric methods: a pilot study, Biomarkers. 22 (2017) 525–536, https://doi.org/10.1080/1354750X.2017.1306753.
[20] S.A. Miller, D.D. Dykes, H.F. Polesky, A simple salting out procedure for extracting DNA from human nucleated cells, Nucleic. Acids. Res. 16 (1988) 1215, https://doi.org/10.1093/nar/16.3.1215.
[21] S. Di Bucchianico, A.R. Gliga, E. Åkerlund, S. Skoglund, I.O. Wallinder, B. Fadeel, H.L. Karlsson, Calcium-dependent cyto- and genotoxicity of nickel metal and nickel oxide nanoparticles in human lung cells, Part. Fibre Toxicol. 15 (2018) 32, https://doi.org/10.1186/s12989-018-0268-y.
[22] C. Rosefort, E. Fauth, H. Zankl, Micronuclei induced by aneugens and clastogens in mononucleate and binucleate cells using the cytokinesis block assay, Mutagenesis. 19 (2004) 277–284, https://doi.org/10.1093/mutage/geh028.
[23] J.C. Ball, A.M. Straccia, W.C. Young, A.E. Aust, The formation of reactive oxygen species catalyzed by neutral, aqueous extracts of NIST ambient particulate matter and diesel engine particles, J. Air Waste Manag. Assoc. 50 (2000) 1897–1903, https://doi.org/10.1080/10473289.2000.10464231.
[24] X. Cao, J. Lintelmann, S. Padoan, S. Bauer, A. Huber, A. Mudan, S. Oeder, T. Adam, S. Di Bucchianico, R. Zimmermann, Adenine derivatization for LC-MS/MS epigenetic DNA modifications studies on monocytic THP-1 cells exposed to reference particulate matter, Anal. Biochem. 618 (2021) 114127, https://doi.org/10.1016/j.ab.2021.114127.
[25] M. Kirsch-Volders, M. Fenech, Inclusion of micronuclei in non-divided mononuclear lymphocytes and necrosis/apoptosis may provide a more comprehensive cytokinesis block micronucleus assay for biomonitoring purposes, Mutagenesis. 16 (2001) 51–58, https://doi.org/10.1093/mutage/16.1.51.
[26] X. Liu, W. Ouyang, Y. Shu, Y. Tian, Y. Feng, T. Zhang, W. Chen, Incorporating bioaccessibility into health risk assessment of heavy metals in particulate matter originated from different sources of atmospheric pollution, Environ. Pollut. 254 (Part B) (2019) 113113, https://doi.org/10.1016/j.envpol.2019.113113.
[27] P. Rossner, H. Libalova, T. Cervena, K. Vrbova, F. Elzeinova, A. Milcova, A. Rossnerova, Z. Novakova, M. Ciganek, M. Pokorna, A. Ambroz, J. Topinka, The processes associated with lipid peroxidation in human embryonic lung fibroblasts, treated with polycyclic aromatic hydrocarbons and organic extract from particulate matter, Mutagenesis. 29 (2019) 153–164, https://doi.org/10.1093/mutage/gez004.
[28] P. Rossner, H. Libalova, K. Vrbova, T. Cervena, A. Rossnerova, F. Elzeinova, A. Milcova, Z. Novakova, J. Topinka, Genotoxicant exposure, activation of the aryl hydrocarbon receptor, and lipid peroxidation in cultured human alveolar type II A549 cells, Mutat. Res. 853 (2020) 503173, https://doi.org/10.1016/j.mrgentox.2020.503173.
[29] P. Thomas, K. Umegaki, M. Fenech, Nucleoplasmic bridges are a sensitive measure of chromosome rearrangement in the cytokinesis-block micronucleus assay, Mutagenesis. 18 (2003) 187–194, https://doi.org/10.1093/mutage/18.2.187.
[30] K. Umegaki, M. Fenech, Cytokinesis-block micronucleus assay in WIL2-NS cells: a sensitive system to detect chromosomal damage induced by reactive oxygen species and activated human neutrophils, Mutagenesis. 15 (2000) 261–269, https://doi.org/10.1093/mutage/15.3.261.
[31] A.K. Prahalad, J. Inmon, L.A. Dailey, M.C. Madden, A.J. Ghio, J.E. Gallagher, Air pollution particles mediated oxidative DNA base damage in a cell free system and in human airway epithelial cells in relation to particulate metal content and bioreactivity, Chem. Res. Toxicol. 14 (2001) 879–887, https://doi.org/10.1021/tx010022e.
[32] P.H. Danielsen, S. Loft, P. Møller, DNA damage and cytotoxicity in type II lung epithelial (A549) cell cultures after exposure to diesel exhaust and urban street particles, Part. Fibre Toxicol. 5 (2008) 6, https://doi.org/10.1186/1743-8977-5-6.
[33] A.F. Dumax-Vorzet, M. Tate, R. Walmsley, R.H. Elder, A.C. Povey, Cytotoxicity and genotoxicity of urban particulate matter in mammalian cells, Mutagenesis. 30 (2015) 621–633, https://doi.org/10.1093/mutage/gev025.
[34] H. Zhao, M.W. Barger, J.K.H. Ma, V. Castranova, J.Y.C. Ma, Cooperation of the inducible nitric oxide synthase and cytochrome P450 1A1 in mediating lung inflammation and mutagenicity induced by diesel exhaust particle, Environ. Health Perspect. 114 (2006) 1253–1258, https://doi.org/10.1289/ehp.9063.
[35] X. Shi, M.J. Keane, O. TM, J. Harrison, S. JE, A. Bugarski, M. Gautam, W. Wallace, Diesel exhaust particulate material expression of in vitro genotoxic activities when dispersed into a phospholipid component of lung surfactant, J. Phys. Conf. Ser. 151 (2009) 012021, https://doi.org/10.1088/1742-6596/151/1/012021.
[36] B.A.M. Bandowe, H. Meusel, Nitrated polycyclic aromatic hydrocarbons (nitro-PAHs) in the environment - A review, Sci. Total Env. 581–582 (2017) 237–257, https://doi.org/10.1016/j.scitotenv.2016.12.115.
[37] P. Rossner, S. Strapacova, J. Stolcpartova, J. Schmuczerova, A. Milcova, J. Neca, V. Vlkova, T. Brzicova, M. Machala, J. Topinka, Toxic effects of the major components of diesel exhaust in human alveolar basal epithelial cells (A549), Int. J. Mol. Sci. 17 (2016) 1393, https://doi.org/10.3390/ijms17091393.
[38] R. Li, L. Zhao, L. Zhang, M. Chen, C. Dong, Z. Cai, DNA damage and repair, oxidative stress and metabolism biomarker responses in lungs of rats exposed to ambient atmospheric 1-nitropyrene, Environ. Toxicol. Pharmacol. 54 (2017) 14–20, https://doi.org/10.1016/j.etap.2017.06.009.
[39] J. Øvrevik, V.M. Arlt, E. Øya, E. Nagy, S. Mollerup, D.H. Phillips, M. Låg, J.A. Holme, Differential effects of nitro-PAHs and amino-PAHs on cytokine and chemokine responses in human bronchial epithelial BEAS-2B cells, Toxicol. Appl. Pharmacol. 242 (2010) 270–280, https://doi.org/10.1016/j.taap.2009.10.017.
[40] T. Cervena, A. Rossnerova, J. Sikorova, V. Beranek, M. Vojtisek-Lom, M. Ciganek, J. Topinka, P. Rossner, DNA damage potential of engine emissions measured in vitro by micronucleus test in human bronchial epithelial cells, Basic Clin. Pharmacol. Toxicol. 121 (2017) 102–108, https://doi.org/10.1111/bcpt.12693.
[41] Y. Shang, Q. Zhou, T. Wang, Y. Jiang, Y. Zhong, G. Qian, T. Zhu, X. Qiu, J. An, Airborne nitro-PAHs induce Nrf2/ARE defense system against oxidative stress and promote inflammatory process by activating PI3K/Akt pathway in A549 cells, Toxicol. Vitr. 44 (2017) 66–73, https://doi.org/10.1016/j.tiv.2017.06.017.
[42] B. Hu, B. Tong, Y. Xiang, S.R. Li, Z.X. Tan, H.X. Xiang, L. Fu, H. Wang, H. Zhao, D.X. Xu, Acute 1-NP exposure induces inflammatory responses through activating various inflammatory signaling pathways in mouse lungs and human A549 cells, Ecotoxicol. Environ. Saf. 189 (2020) 109977, https://doi.org/10.1016/j.ecoenv.2019.109977.
[43] M. Fenech, M. Kirsch-Volders, A.T. Natarajan, J. Surralles, J.W. Crott, J. Parry, H. Norppa, D.A. Eastmond, J.D. Tucker, P. Thomas, Molecular mechanisms of micronucleus, nucleoplasmic bridge and nuclear bud formation in mammalian and human cells, Mutagenesis. 26 (2011) 125–132, https://doi.org/10.1093/mutage/geq052.
[44] I.W. Jarvis, C. Bergvall, M. Bottai, R. Westerholm, U. Stenius, K. Dreij, Persistent activation of DNA damage signaling in response to complex mixtures of PAHs in air particulate matter, Toxicol Appl Pharmacol. 266 (2013) 408–418, https://doi.org/10.1016/j.taap.2012.11.026.
[45] N. Jariyasopit, M. McIntosh, K. Zimmermann, J. Arey, R. Atkinson, P.H. Cheong, R.G. Carter, T.W. Yu, R.H. Dashwood, S.L. Massey Simonich, Novel nitro-PAH formation from heterogeneous reactions of PAHs with NO2, NO3/N2O5, and OH radicals: prediction, laboratory studies, and mutagenicity, Environ Sci Technol. 48 (2014) 412–419, https://doi.org/10.1021/es4043808.
[46] C. Walgraeve, K. Demeestere, J. Dewulf, R. Zimmermann, H. Va. Langenhove, Oxygenated polycyclic aromatic hydrocarbons in atmospheric particulate matter: Molecular characterization and occurrence, Atmospheric Environment. 44 (2010) 1831–1846, https://doi.org/10.1016/j.atmosenv.2009.12.004.